



HAL
open science

Energy Variance of a Quantum Bit

Gilbert Reinisch

► **To cite this version:**

| Gilbert Reinisch. Energy Variance of a Quantum Bit. 2022. hal-03628136v1

HAL Id: hal-03628136

<https://hal.science/hal-03628136v1>

Preprint submitted on 1 Apr 2022 (v1), last revised 6 May 2022 (v2)

HAL is a multi-disciplinary open access archive for the deposit and dissemination of scientific research documents, whether they are published or not. The documents may come from teaching and research institutions in France or abroad, or from public or private research centers.

L'archive ouverte pluridisciplinaire **HAL**, est destinée au dépôt et à la diffusion de documents scientifiques de niveau recherche, publiés ou non, émanant des établissements d'enseignement et de recherche français ou étrangers, des laboratoires publics ou privés.

Energy Variance of a Quantum Bit

Gilbert Reinisch*

*Université de la Côte d'Azur - Observatoire de la Côte d'Azur
06304 Nice Cedex - France*

and†

*Science Institute, University of Iceland,
Dunhaga 3, IS-107 Reykjavik, Iceland*

Abstract

We show that the energy spectrum of a driven two-level quantum system —or driven quantum bit (qubit)— can be mathematically defined by its two “state energies” as the time derivatives of its large-amplitude, high-frequency internal as well as overall phases. While the mean values of these latter do fit of course Rabi’s well-known harmonic (weak drive) as well as anharmonic (strong drive) dynamics, the standard deviations of these both state energies may become comparable to their mean values themselves. This remarkable property, which we check by use of the quantum expectation value of the variance operator, defines a large statistical time-dependent range of available values for the qubit energy in the presence of an external perturbation. We take the example of a recent experiment [*Z. Minev et al. Nature, 570, 200 (2019)*] and recover by use of the present theory the measured “time-of-flight” values.

PACS numbers: 02.60.Lj 12.20.Ds 73.21.La

*Electronic address: Gilbert.Reinisch@oca.eu

†Electronic address: gilbert@hi.is

A. Introduction

In the normalized $|a, b\rangle$ two-state base, the Schrödinger equation:

$$i\hbar \frac{d}{dt} \Psi = \mathbf{H} \Psi \quad (1)$$

where the normalized spinor wavefunction and the Hamiltonian are respectively:

$$\Psi(t) = \begin{pmatrix} \psi_a(t) \\ \psi_b(t) \end{pmatrix} \quad ; \quad \mathbf{H}(t) = \begin{pmatrix} \mathcal{E}(t) & K \\ K & -\mathcal{E}(t) \end{pmatrix} \quad (2)$$

defines by use of the two Pauli matrices σ_x and σ_z the two-level quantum system (or qubit) in the presence of the external time-dependent energy drive $\mathcal{E}(t)$ and the off-diagonal constant K . The quantum expectation values of the energy and the variance are respectively:

$$\mathbf{E}(t) = \langle \Psi(t) | \mathbf{H}(t) | \Psi(t) \rangle. \quad (3)$$

and:

$$\mathbf{V}(t) = \langle \Psi(t) | \mathcal{V}(t) | \Psi(t) \rangle. \quad (4)$$

where this latter is defined by the following Hermitian variance operator:

$$\mathcal{V}(t) = [\mathbf{H}(t) - \mathbf{E}(t)]^2. \quad (5)$$

The resulting standard deviation of the energy with respect to its mean-value (3) provides a useful theoretical frame when considering measurement processes of the qubit state. In particular, a quasi-continuous measurement process, known to yield the quantum Zeno effect (QZE) [1] [2], can be accurately described within such a standard deviation [3]. It yields the sharp quantum transitions which have been observed in a recent experiment [4]. Inasmuch as the present theory does not depend on the specific measurement process—contrary to [4] where the particular $|G\rangle$, $|D\rangle$ and $|B\rangle$ three-level quantum system is explicitly taken into account—it has a broad audience and concerns every quasi-continuously observed qubit, whatever the way the two states are actually measured. By first-principle heuristic arguments and without a detailed dynamical analysis as in [3], we illustrate here this universal approach by use of the two following state energies $E_{a,b}(t)$ that are defined in accordance with Eqs. (2-3):

$$\mathbf{E}(t) = |\psi_a(t)|^2 E_a(t) + |\psi_b(t)|^2 E_b(t). \quad (6)$$

B. Hamiltonian dynamical system (HDS) description of a driven qubit

Together with the well-known spin-one-half system, the Josephson junction is the paradigm of the spinor quantum-mechanical description (1-2) [5]. Then the two state wavefunction components $\psi_{a,b}$ are the Ginzburg–Landau order parameters of the two superconductors separated by the weak link between them. They can be written:

$$\psi_a(t) = \sqrt{\frac{1 + \alpha(t)}{2}} e^{i\Theta(t)} \quad ; \quad \psi_b(t) = \sqrt{\frac{1 - \alpha(t)}{2}} e^{i[\Theta(t) + \delta(t)]}. \quad (7)$$

In (7), the variable $\delta(t)$ is the phase difference of the Ginzburg-Landau order parameters across the junction. It is called the Josephson phase. The normalized charge carrier densities

of each superconductor, namely $[1 \pm \alpha(t)]/2$, are both defined by the single variable $\alpha(t)$. If the above system is regarded as a spin one-half, its angular positions θ and ϕ on the Bloch sphere are straightforward, according to:

$$\alpha = \cos \theta \quad ; \quad \phi = \Theta + \frac{\delta}{2}. \quad (8)$$

Then:

$$\psi_a(t) = e^{i\phi(t)} \cos \frac{\theta(t)}{2} e^{-i\delta(t)/2} \quad ; \quad \psi_b(t) = e^{i\phi(t)} \sin \frac{\theta(t)}{2} e^{+i\delta(t)/2}. \quad (9)$$

It has been shown in [6] [7] that δ and α are the conjugate canonical coordinates in the following Hamiltonian formulation of classical-like mechanics:

$$\dot{\alpha} = -\frac{\partial \mathcal{H}}{\partial \delta} = \sqrt{1 - \alpha^2} \sin \delta \quad ; \quad \dot{\delta} = \frac{\partial \mathcal{H}}{\partial \alpha} = -\frac{\alpha}{\sqrt{1 - \alpha^2}} \cos \delta + \mathcal{E}(\tau), \quad (10)$$

where the Hamiltonian is:

$$\mathcal{H} = \sqrt{1 - \alpha^2} \cos \delta + \alpha \mathcal{E}(\tau). \quad (11)$$

In the above Hamiltonian dynamical system (HDS), the dot means the derivation with respect to the dimensionless time $\tau = \Omega t$ defined by $\Omega = 2K/\hbar$ (e.g. it is the Larmor frequency of a two-level spin one-half system). Hence we assume in the present work:

$$K = 1 \quad ; \quad \hbar = 2 \quad ; \quad \Omega = 1. \quad (12)$$

Note that the time-dependent overall phase $\Theta(\tau)$ in (7) is *not* a 3rd independent variable: it is slaved to the solution of HDS (10-11) by:

$$\dot{\Theta} = -\frac{1}{2} \left[\sqrt{\frac{1 - \alpha}{1 + \alpha}} \cos \delta + \mathcal{E}(\tau) \right]. \quad (13)$$

Contrary to intuitive opinions, the dynamics of the overall phase of a quantum state can indeed yield an observable physical effect (e.g. it causes the famous 4π -symmetry of spinor wave functions that have been directly verified in both division-of-amplitude [8][9] and division-of-wave-front [10] neutron interferometry experiments). When $\alpha \equiv 0$ (which is Feynman's basic assumption [5] for the description of the stationary Josephson effect), Eqs. (10) yield the two Josephson equations (\mathcal{E} is then the applied voltage).

In the simplest conservative case $\mathcal{E} \equiv 0$, the classical-like HDS orbits defined by Hamilton equations (10) do all have the same reduced frequency $+1$ (actually $+\Omega$) for $\mathcal{H} > 0$ (resp. -1 , or $-\Omega$, for $\mathcal{H} < 0$). They define the corresponding quantum superposition states of the system in agreement with Eqs. (7) and (13) [6]. Such a binary structure of the orbit frequency, namely $\pm\Omega$ in actual units, is the translation in terms of the HDS equations of motion (10-11) and action [3], of the eigenvalues ± 1 in the two-level energy spectrum of the undriven qubit. In the driven, however still conservative case $\mathcal{E} \equiv \text{constant} \neq 0$, all the orbits do still keep the same angular frequency $\pm\sqrt{1 + \mathcal{E}^2}$ (actually the corresponding eigenvalues), depending on the sign of \mathcal{H} . Moreover it has been shown in [6] that the above-mentioned 4π symmetry of the overall qubit phase Θ becomes an immediate consequence of the HDS solution (13).

We have in accordance with Eqs. (2), (3), (7) and (11) the following fundamental link between the mean qubit energy \mathbf{E} and the HDS energy \mathcal{H} in the dimensionless units (12):

$$\mathbf{E}(\tau) = \mathcal{H}(\tau). \quad (14)$$

C. Time-dependent state energies $E_{a,b}(\tau)$ and variance $\sigma_{a,b}^2(\tau)$

Equations (6-7) and (14) yield the following HDS definition of the two qubit's time-dependent *state energies* in the dimensionless units (12):

$$E_a = \frac{\mathcal{H} + \mathcal{E}}{1 + \alpha} \quad ; \quad E_b = \frac{\mathcal{H} - \mathcal{E}}{1 - \alpha}. \quad (15)$$

They are the derivatives of the two internal as well as overall phases $\delta(\tau)$ and $\Theta(\tau)$:

$$E_a = -\hbar \frac{d\Theta}{dt} = -2\dot{\Theta} \quad ; \quad E_b = -\hbar \frac{d(\Theta + \delta)}{dt} = -2(\dot{\Theta} + \dot{\delta}), \quad (16)$$

by use of Eqs. (10) and (13). They provide an explicit fine-structure mapping of the dynamical properties of the classical-like HDS trajectories (10-11) to the mean quantum energy (6) and to the variance:

$$\sigma_{a,b}^2(\tau) = |\psi_{a,b}(\tau)|^2 [E_{a,b}(\tau) - \mathcal{H}(\tau)]^2, \quad (17)$$

in terms of the standard deviations $\pm\sigma_{a,b}(\tau)$. The necessary link with the quantum variance (4-5) is performed as follows. Using (14), we have:

$$\mathcal{V} = \begin{pmatrix} (\mathcal{H} - \mathcal{E})^2 + K^2 & -2KH \\ -2KH & (\mathcal{H} + \mathcal{E})^2 + K^2 \end{pmatrix}, \quad (18)$$

and therefore, by use of Eqs. (4) and (7):

$$\mathbf{V} = (1 - 2K)\mathcal{H}^2 + 2(K - 1)\alpha\mathcal{E}\mathcal{H} + \mathcal{E}^2 + K^2. \quad (19)$$

Since we assume $K = 1$ in accordance with (12), Eq. (20) becomes:

$$\mathbf{V} = \mathcal{E}^2 - \mathcal{H}^2 + 1 \sim 1 - \mathcal{H}^2, \quad (20)$$

if the qubit is weakly Rabi-driven as envisaged in the next section.

D. Weakly resonant Rabi-driven case

When the weak resonant field:

$$\mathcal{E}(\tau) = A \sin \tau \quad ; \quad A \ll 1, \quad (21)$$

is applied to the system, we obtain in accordance with Eq. (11) the well-known quasi-harmonic Rabi oscillation between the two eigenvalues ± 1 of the mean energy:

$$\mathcal{H} \sim \cos \frac{A\tau}{2} + \Delta\mathcal{H} \quad ; \quad \Delta\mathcal{H} = \alpha\mathcal{E}(\tau) = A\alpha \sin \tau \ll 1. \quad (22)$$

One obtains a regime of HDS quasiperiodic orbits slowly spiraling out of one $\mathcal{H} = \pm 1$ eigenvalue og in to the next $\mathcal{H} = \mp 1$ one [7]. The corresponding ‘‘dressing’’ of the quasi-harmonic mean energy value (22) by the standard deviations defined by variance (17) is

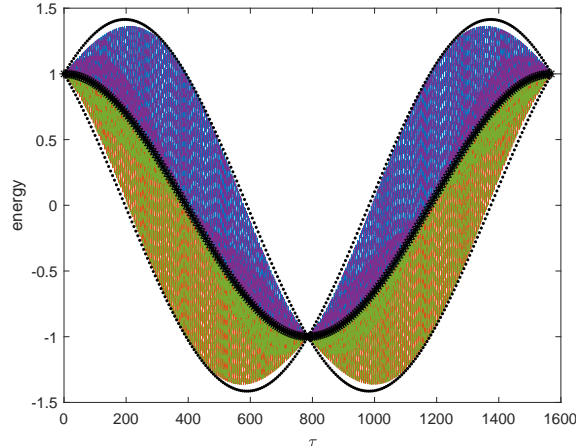


FIG. 1: Validation of the state-energy description (15-17) by use of the variance Hermitian operator (4-5) for $A = 8 \cdot 10^{-3}$. The qubit's colored available energy region is defined by the standard deviation dressing (17) of Rabi's quasi-harmonic HDS Hamiltonian—or mean energy—(22) during one Rabi period $4\pi/A = 1571$ in reduced units (12) (thick black plot). Dotted black plot: the quantum standard deviations about \mathcal{H} as defined by quantum variance (20).

quite spectacular [3]. In Fig. 1, $\mathcal{H}(\tau)$ is displayed by the thick black plot while the quantum standard deviations about it, defined by quantum variance (20), are shown by the dotted black plots. The quite dense colored patterns are built from the oscillatory standard deviations (17) with extremely small HDS orbit period $\sim 2\pi \ll 1571$ at the scale of the Rabi period $4\pi/A = 1571$. The energy standard deviations $+\sigma_a(\tau)$ (continuous purple) and $-\sigma_a(\tau)$ (continuous green) due to state energy $E_a(\tau)$ defined in (15) are phase-shifted by $\sim \pi$ with respect to the standard deviations $+\sigma_b(\tau)$ (dotted purple) and $-\sigma_b(\tau)$ (dotted green) due to state energy $E_b(\tau)$. All these high-frequency standard deviations display the rather important dispersion of the qubit acceptable energy values about its mean value \mathcal{H} except at the two eigenvalues ± 1 where, as expected, this dispersion vanishes. We note with interest that these standard deviation patterns are quite accurately bounded by the quantum standard deviations defined by quantum variance (20). Therefore this remarkable property establishes the necessary statistical link between the variance Hermitian operator (4-5) and the state-energy description (15-17). It validates this latter.

E. Quantum Zeno jump

The measured “time-of-flight” values obtained by a continuous measurement process in experiment [4] have been recovered in the frame of the above theory by considering the quantization of the HDS action [3]. Here we wish to show that these values are actually an immediate first-principle consequence of Fig. 1 and—contrary to the quantum trajec-

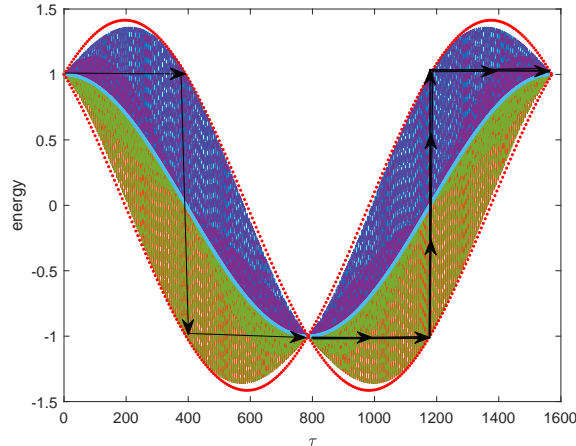


FIG. 2: $A = 8 \cdot 10^{-3}$: the qubit’s available energy region defined by Fig. 1 together with its quasi-harmonic HDS Hamiltonian \mathcal{H} (in continuous blue) and its quantum standard deviations (20) about \mathcal{H} (red dotted plots). The general principle of a step-like quantum jump due to repetitive eigenstate measurements is illustrated by arrows. The thick arrows display the Rabi-stimulated energy jump occurring at $\tau = 1183$ (actually at $\mathcal{H} = 0$) from the ground state $E = -1$ to the excited level $E = +1$. The thinner path displays the de-excitation reverse process.

tory explanation given in [4]— they do not depend on the specific continuous measurement process (provided this latter is long-lasting enough). Indeed *any* such process yields QZE “freezing” of the corresponding quantum states in their initial configuration [1] [2] and this latter remains possible as long as the resulting trajectory lies inside of the qubit’s available energy region defined by Fig. 1.

Let us be specific and consider Fig. 2. Assume that the system, while still resonantly Rabi-driven, is initially in, say, its ground state -1 (i.e. at half the Rabi period $\tau = 785$) and introduce a repetitive measurement process in accordance with [2] or, equivalently, with [4] (the following applies as well if we choose the excited state: see Fig. 2 at $\tau = 0$). Then, due to QZE which acts as a *strong perturbation*, the system is forced to remain “frozen” in this lowest energy value instead of entering Rabi’s standard unperturbed harmonic excitation dynamics (22) displayed by the blue line. Consequently, its energy keeps its value -1 along the horizontal segment as τ increases for $785 < \tau < 1183$ (lowest horizontal arrow path), i.e. as long as the energy of the system stays within the statistically accessible energy region defined by Eq. (17) or equivalently by Eq. (20) (dotted red line). When reaching this boundary at $\tau = 1183$, it jumps to the excited level $+1$ in accordance with the vertical arrow path in order to continue the QZE state freezing process from $\tau = 1183$ to $\tau = 1571$ if the repetitive measurement is lasting over a time interval greater than this half Rabi period. This QZE jump —which we call “*quantum Zeno jump*” (QZJ)— actually absorbs at once all the energy input due to the external Rabi drive that has been accumulated by the system during its forced QZE freezing stage.

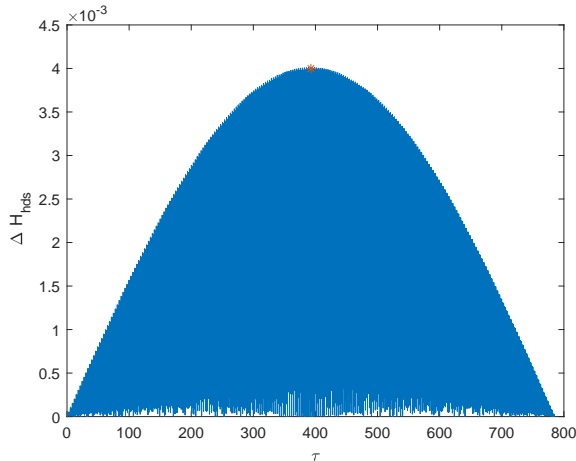


FIG. 3: The quasi-stochastic energy input $\Delta\mathcal{H}$ defined by Eq. (22) over half a Rabi period $2\pi/A$ when the origin of time is now taken at $\tau = 785$ in Figs. 1-2. Its seemingly two-dimensional dense pattern results from its extremely fast oscillations at the scale of the Rabi period. Therefore it will be regarded as the uncertainty in the energy input at a given time τ . The star indicates the maximum at $\tau = 393$ or $\mathcal{H} = 0$ that scales this uncertainty in (23).

The above QZJ scheme is oversimplified. Indeed the standard deviation boundary at $\tau = 1183$ is only statistical: it has not a precise definite value. Therefore the QZJ may occur at any time in the interval $\Delta\tau$ about $\tau = 1183$. When trying to evaluate it, one should regard the Hamiltonian driving term $\Delta\mathcal{H}$ in (22) as a quasi-stochastic energy input, as shown by Fig. 3. Indeed, $\Delta\mathcal{H}$ oscillates extremely rapidly at the scale of the Rabi period $4\pi/A$. It actually looks like a mere two-dimensional uniformly dense drive term pattern and thus yields the corresponding time interval $\Delta\tau$

$$\Delta\mathcal{H}\Delta\tau \geq \frac{\hbar}{2} = 1, \quad (23)$$

in which any step-like QZJ illustrated by Fig. 2 can statistically occur (cf. our choice (12) of the reduced units). Since the QZJ formerly appears at half the gap defined by $\mathcal{H} = 0$ (cf. Fig. 2), we take $\Delta\mathcal{H} = \Delta\mathcal{H}_{max} = 4 \cdot 10^{-3}$ in (23) —see the star in Fig. 3— and therefore $\Delta\tau_{min} \sim 1/\Delta\mathcal{H}_{max} \sim 250$. This time interval is pictured by the two vertical bars in Fig. 4 where the experimental data given in Fig. 3b of Ref. [4] are reproduced by use of red circles, using for the normalization of our τ -axis the experimental Rabi period $T_{Rabi} = 50 \mu s$ given in [4] (their $\sim 13\%$ deviation from the excited eigenvalue $+1$ is due, the authors say, to imperfections, mostly excitations to higher levels). We see that $\Delta\tau_{min} \sim 250$ fairly agrees with the so-called “time-of-flight” value $\sim 2\Delta_{mid}$ defined in Fig. 3b of [4]. Moreover, $\Delta\tau_{min}$ is also in good agreement with HDS action quantization when the system crosses the separatrix of the system at $\mathcal{H} = 0$ [3]. Note that the l.h.s. of inequality (23) has indeed the dimension of an action.

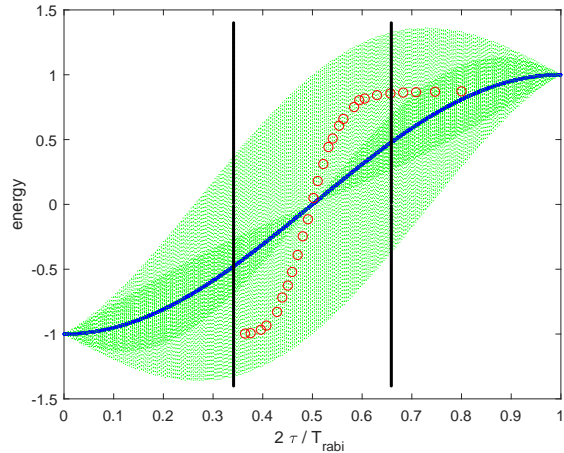


FIG. 4: Second (r.h.s.) part of Figs. 1-2 illustrating the *QZE-vs-Rabi* excitation process (quantum Zeno jump, or QZJ). Blue plot: Rabi's mean energy defined by Eq. (22). Circles: the path in the Hilbert space followed by the jump evolutions given in Fig. 3b of Ref. [4], using its $T_{Rabi} = 50 \mu s$ Rabi period for the normalization of the τ -axis. The 13% deviation from the excited eigenvalue $+1$ is due to imperfections, mostly excitations to higher levels [4]. The two vertical bars display the minimum duration $\Delta\tau_{min}$ of the transition obtained as the consequence of the uncertainty principle (23) when the perturbation $\Delta\mathcal{H}$ illustrated by Figs 3 is maximum (star) .

F. Conclusion

One important point in the above QZJ statistical description (23) and illustrated by Figs. 2-4 is that we recover the undeterministic dynamical scheme of a quantum jump à-la-Bohr. Contrary to [4], the present theory does not claim to deterministically describe the reality of the quantum jump. It only tells the observer that, due to the repetitive measurement process and to the general qubit energy variance properties displayed by Fig. 1, the system may statistically undergo a sudden transition about half gap at any time within that interval $\Delta\tau_{min}$ which is defined by the uncertainty principle. As such, it is generic and does not depend on the particular continuous qubit measurement process —by contrast with [4] where the specific $|G\rangle$, $|D\rangle$ and $|B\rangle$ three-level quantum system is explicitly taken into account. Therefore it provides a physical frame in which *all* particular qubit measurement processes —provided they are repetitive and long-lasting enough— must fit.

A second important consequence concerns strong Rabi qubit driving. While the HDS definition of the energies $E_{a,b}$ still remains valid, their statistical variance and/or standard deviation statistical properties become useless because their spectrum may appear either chaotic or discrete. In this latter case, it is defined by the existence of phase-locked cycles in the solution of the HDS differential system. Then the state energies $E_{a,b}$ provide an interesting tool for the description of the corresponding qubit frequency comb in such strongly

perturbed cases [11].

- [1] B. B. Misra and E. Sudarshan, *J. Math. Phys.* **18**, 756 (1977).
- [2] W. Itano, *Current Science* **116**, , 201 (2019).
- [3] G. Reinisch, *Results Phys* **29**, 104761 (2021), doi.org/10.1016/j.rinp.2021.104761.
- [4] Z. Mineev, S. Mundhada, S. Shankar, P. Reinhold, R. Gutiérrez-Jáuregui, R. Schoelkopf, M. Mirrahimi, H. Carmichael, and M. Devoret, *Nature* **570**, 200 (2019).
- [5] R. Feynman, R. Leighton, and M. Sands, *The Feynman Lectures on Physics* (Addison-Wesley, 1965).
- [6] G. Reinisch, *Physica D* **119**, 239 (1998).
- [7] G. Reinisch, *Phys. Lett. A* **238**, 107 (1998).
- [8] H. H. Rauch, A. Zeilinger, G. Badurek, A. Wilting, W. Bauspiess, and U. Bonse, *Phys. Lett. A* **54**, 425 (1975).
- [9] S. Werner, R. Colella, A. Overhauser, and C. Eagen, *Phys. Rev. Lett.* **35**, 1053 (1975).
- [10] A. Klein and G. Opat, *Phys. Rev. Lett.* **37**, 238 (1976).
- [11] G. Reinisch, *Results Phys* **33**, 105136 (2022), doi.org/10.1016/j.rinp.2021.105136.

Acknowledgments

The author gratefully acknowledges financial and technical support from UMR *Lagrange* (Observatoire de la Côte d’Azur, université de Nice, France) as well as from the Icelandic Technology Development Fund (University of Iceland, Reykjavik, Iceland).